Computers and Electronics in Agriculture 89 (2012) 145–157

Contents lists available at SciVerse ScienceDirect

Computers and Electronics in Agriculture

journal homepage: www.elsevier.com/locate/compag

Using vegetation index and modified derivative for early detection of soybean plant injury from glyphosate

Haibo Yao [a,*], Yanbo Huang [b], Zuzana Hruska [a], Steven J. Thomson [b], Krishna N. Reddy [b]

[a] Mississippi State University, Geosystems Research Institute, Stennis Space Center, MS, USA
[b] United States Department of Agriculture, Agricultural Research Service, Crop Production Systems Research Unit, Stoneville, MS, USA

ARTICLE INFO

Article history:
Received 24 May 2012
Received in revised form 31 July 2012
Accepted 2 September 2012

Keywords:
Reflectance
Crop injury
Vegetation index
Derivatives
Soybean
Glyphosate

ABSTRACT

Glyphosate is a non-selective, systemic herbicide highly toxic to sensitive plant species. Its use has seen a significant increase due to the increased adoption of genetically modified glyphosate-resistant crops since the mid-1990s. Glyphosate application for weed control in glyphosate-resistant crops can drift onto an off-target area, causing unwanted injury to non-glyphosate resistant plants. Thus, early detection of crop injury from off-target drift of herbicide is critical in crop production. In non-glyphosate-resistant plants, glyphosate causes a reduction in chlorophyll content and metabolic disturbances. These subtle changes may be detectable by plant reflectance, which suggests the possibility of using optical remote sensing for early detection of drift damage to plants. In order to determine the feasibility of using optical remote sensing, a greenhouse study was initiated to measure the canopy reflectance of soybean plants using a portable hyperspectral image sensor. Non-glyphosate resistant soybean (*Glycine max* L. Merr.) plants were treated with glyphosate using a pneumatic track sprayer in a spray chamber. The three treatment groups were control (0 kg ae/ha), low dosage (0.086 kg ae/ha), and high dosage (0.86 kg ae/ha), each with four 2-plant pots. Hyperspectral images were taken at 4, 24, 48, and 72 h after application. The extracted canopy reflectance data was analyzed with vegetation indices. The results indicated that a number of vegetation indices could identify crop injury at 24 h after application, at which time visual inspection could not distinguish between glyphosate injured and non-treated plants. To improve the results a modified method of spectral derivative analysis was proposed and applied to find that the method produced better results than the vegetation indices. Four selected first derivatives at wavelength 519, 670, 685, and 697 nm could potentially differentiate crop injury at 4 h after treatment. The overall false positive rate was lower than the vegetation indices. Furthermore, the derivatives demonstrated the ability to separate treatment groups with different dosages. The study showed that hyperspectral imaging of plant canopy reflectance could be a useful tool for early detection of soybean crop injury from glyphosate, and that the modified spectral derivative analysis had a better performance than vegetation indices.

1. Introduction

During routine herbicide applications, herbicide drift can occur when herbicide particles move onto off-target areas under weather conditions that are favorable for drift. When the herbicide lands on the off-target plant surfaces, unwanted plant damage can occur. Thus, in herbicide applications, one of the main objectives is to minimize off-target drift that may result in injury to other crops. This task can be implemented through proper training, careful planning of herbicide applications, good maintenance of equipment, and field experience. However, when drift does occur, it is important to be able to detect the onset of the crop injury due to herbicide drift, and preferably be able to determine the relationship between the crop injury and dosage. In the past decade, one herbicide, glyphosate, has been widely adopted for weed management in agricultural fields due to the increased utilization of genetically modified crops that are resistant to glyphosate. Glyphosate is a non-selective herbicide used for control of weeds before planting crops and postemergence (POST) applications in genetically modified GR (glyphosate-resistant) crops. Glyphosate use has seen a significant increase. For example, the amount of glyphosate (Active Ingredient) on all soybean crops in the US has increased from 4896 (thousand lb) in 1996 to 96,725 (thousand lb) in 2006 (Center for Food Safety, 2008).

Glyphosate is highly active on sensitive plant species even at low doses. Once applied, the inhibition of plant growth is immediate due to the depletion of aromatic amino acids essential for plant growth. In addition to growth reduction, glyphosate causes chlorosis and necrosis. The consequence is yield reduction or complete

* Corresponding author. Address: Mississippi State University, Geosystems Research Institute, 1021 Balch Boulevard, Stennis Space Center, MS 39529, USA. Tel.: +1 228 688 3742; fax: +1 228 688 7100.
E-mail address: haibo@gri.msstate.edu (H. Yao).

0168-1699/$ - see front matter © 2012 Elsevier B.V. All rights reserved.
http://dx.doi.org/10.1016/j.compag.2012.09.001

destruction of a susceptible plant. Glyphosate is usually applied to foliage through ground or aerial applications. Typical applications include postemergence application for weed control. For instance, glyphosate is normally applied in GR soybean fields for weed control in the early growth season. However weather conditions during this period of time in the year are normally windy (depends on location, Henry et al., 2004), and this increases the possibility of glyphosate drift. Glyphosate drift onto non-target crops is common in agricultural regions. The drift to non-GR crops may cause injury and reduce yields. When drift occurs, farmers are interested in the coverage and extent of the drift damage in order to project the severity of unintended injury as early as possible. With this information farmers can take appropriate actions to best protect their interests. Such actions include replanting or seeking insurance compensation. Thus, the study of glyphosate drift is important to the farming industry. Stated another way, an early warning system for herbicide drift detection in weed management would greatly benefit farmers.

A number of injury identification methods have been evaluated on crops injured by off-target drift of glyphosate. Typically, visual examination provides a way to assess drift occurrence and extent of injury. This approach is possible when injury is obvious to the naked eye. In this case, aerial photography can be used to aid in detection over large areas. Another approach to assess severity of plant damage is to measure physical factors such as plant height (Rowland, 2000) and/or by measurement of chlorophyll and shikimate levels (Reddy et al., 2010; Ding et al., 2011a). Above all, these methods can provide damage assessment when the injury is obvious, well after application (7–14 days after the drift incident). These damage assessment methods are tedious and cause delay in early critical decision-making. Alternative approaches for early warning/detection of glyphosate drift damage would be highly desirable.

In the injury process, glyphosate also causes a reduction in chlorophyll content, decreases in photosynthetic rate, nitrate reductase activity, and nitrogen fixation and accumulation (Bellaloui et al., 2006). These changes in the plant may be detectable by plant reflectance measurements before symptoms of injury become visible. This suggests the possibility of using sensitive, optical remote sensing for early detection of drift damage to plants. Several remote sensing methods have been developed previously in an attempt to detect crop injury due to herbicide drift. The methods include multispectral imaging (Thelen et al., 2004; Huang et al., 2010), fiber optic-based spectral reflectance measurements (Henry et al., 2004; Huang et al., 2012), and chlorophyll fluorescence measurements (Huang et al., 2012). Among them the chlorophyll fluorescence method is not suitable for rapid and early detection, as its measurement requires direct contact against a small section of the plant leaves for a period of time.

The multispectral imaging approach (Thelen et al., 2004; Huang et al., 2010) used imagery with several broadband reflectance measurements including at least a red and a near-infrared band. The multispectral images could provide good spatial resolution in the data. However, the broadband multispectral imagery lacks spectral resolution in the reflectance measurement, and standard bands customarily assigned to multispectral systems are not necessarily appropriate for optimal damage detection. Consequently, a major drawback of this method is that the fine spectral reflectance feature of a plant at the red edge ($\sim$700 nm) of the electromagnetic spectrum range cannot be explored. The red edge is an important spectral range for plant vigor and stress monitoring.

The fiber optic-based method (Henry et al., 2004; Huang et al., 2012) provides an opportunity for narrowband reflectance measurements. The narrowband reflectance has the capability of revealing subtle changes in plant reflectance, which could present more useful information in detecting the onset of crop injury. However, the fiber optic-based reflectance measurement lacks spatial information in the data. It is a single point measurement of the plant. The reflectance data is a mixed signal of all the reflectance within the fiber's field of view. Huang et al. (2012) avoided the spectral mixture problem by pointing the optical fiber directly over a single leaf. However this approach limited the viewing area. Canopy reflectance, which is crucial for crop stress detection, could not be measured in this way. To better differentiate various plant parts and background, it is desirable to use spectral data with both high spatial and spectral resolution. In this case, an imaging spectrometer or hyperspectral imaging system (Yao et al., 2008) can be used to provide such high quality data. Hyperspectral imaging systems have been widely used in agriculture applications, with data from space-borne (Gong et al., 2003), airborne (Yao and Tian, 2003), and terrestrial-based platforms (Ye et al., 2008).

When using hyperspectral image data for vegetation and plant monitoring, vegetation index (VI) is widely applied. Many vegetation indices have been used in different applications. Among them, the most important vegetation index is the Normalized Difference Vegetation Index (NDVI) (Rouse et al., 1973) calculated by using the data at the red and near infrared wavelengths. Hyperspectral images make it possible to build more refined vegetation indices by using distinct narrow-bands. A common practice in calculating hyperspectral indices is the use of individual image bands. For most of the time one specific image band pair is selected based on crop characteristics. For example, one study (Haboudane et al., 2002) used CASI (Compact Airborne Spectral Imager) images to calculate VIs. Image bands centered at 550, 670, 700, and 800 nm were used to calculate several vegetation indices for crop chlorophyll content prediction. The reason for selecting 700 nm was because it is located at the edge between the region where vegetation reflectance is dominated by pigment absorption and the beginning of the red edge region where reflectance is more influenced by the structural characteristics of the vegetation. To apply VIs for glyphosate injury detection on soybean plant, Huang et al. (2012) used 4 VIs, NDVI, RVI (Ratio Vegetation Index), SAVI (Soil Adjusted Vegetation Index), and DVI (Difference Vegetation Index). It was found that crop stress due to glyphosate injury could be detected 24 h after application. However this data was based on spectral measurements over part of a single leaf instead of using canopy reflectance.

Derivative analysis is another approach to analyze hyperspectral data (Thorp et al., 2004). Derivative analysis is promising for use with remote sensing data (Tsai and Philpot, 1998). Higher order derivatives should be relatively insensitive to illumination variations, especially with hyperspectral data, due to its small spectral sampling interval. The most commonly used derivatives are first and second order. Since derivative analysis is quite sensitive to noise, spectral data smoothing is normally applied. Examples of the filtering techniques include Savitzky–Golay filtering and mean low-pass filtering. One study (Smith et al., 2004) suggested that derivative analysis in the red edge range (690–750 nm) could be used for plant stress detection. However, another study (Estep and Carter, 2005) found that when certain derivatives were used for plant nitrogen and water stress detection, there was no advantage of using the derivatives compared to narrow-band vegetation indices. The study used AVIRIS (Airborne Visible/Infrared Imaging Spectrometer) data over corn plots having different nitrogen fertilization treatments. The applied first derivatives were at 495, 568, 696, 982, and 1025 nm. Since these wavelengths were pre-defined from other literature, they might not be suitable for all applications.

This paper utilized a high resolution portable hyperspectral imaging system to study glyphosate damage on soybean plants. The study was conducted in a greenhouse to evaluate crop canopy reflectance data for the detection of crop injury caused by applied glyphosate. The objectives of this study were, to determine the effectiveness of canopy reflectance for detecting the onset of crop injury caused by applied glyphosate, and to propose and develop a modified derivative analysis method for crop stress detection.

2. Materials and methods

2.1. Hyperspectral imaging system

The visible near-infrared hyperspectral imaging system (Fig. 1) includes a 14-bit PCO1600 CCD (charge-coupled device) high resolution camera from the Cooke Corporation (Romulus, MI, USA), an ImSpector V10E spectrograph (Spectral Imaging Ltd., Oulu, Finland) with a 30 μm entrance slit, and a 23 mm Schneider lens. The effective wavelength range is 400–900 nm. The PCO1600 camera has a CCD with resolution of 1600×1200 pixels and is thermoelectrically cooled. Image data transfer from the camera to the computer is through an IEEE 1394 "firewire" link. The system uses push-broom line scanning. It scans an input image within the focal plane of a front lens and disperses an input image line (via the spectrograph) vertically as a function of the spectral wavelengths. In order to move the front lens for the focal plane line scanning, the system utilized a linear motor (Model Stage A-10 motor with a NCS-1S Motor controller, Newmark Systems Inc., Mission Viejo, CA) for internal scanning. Thus, there is no need for additional linear stage to move the target. In order to illuminate the target area in the in-door environment, two mr16 tungsten halogen bulbs with dichroic reflectors are mounted with the sensor on an adjustable camera stand. The lamps are fitted with diffusion and color-balancing filters in order to resolve specular reflectance and to simulate natural lighting.

2.2. Experiment configuration and design

This experiment was conducted in a greenhouse environment at the Crop Production Systems Research unit, USDA-ARS, Stoneville, MS. A total of 12 pots of non-glyphosate-resistant soybeans (cultivar SO80120LL) plants raised in pots were used. There were two plants per pot. The pots remained in the greenhouse throughout the experiment. The soybean plants were subjected to glyphosate treatments 4 weeks after planting (at three-trifoliolate leaf stage). Four plants received low dose treatment (0.086 kg ae/ha), and four high dose treatment (0.86 kg ae/ha). The remaining four plants were used as controls (no treatment). One application of the predetermined treatment was applied in a spray chamber (Ding et al., 2011b). Specifically, in the spray chamber a TeeJet 8002E nozzle (TeeJet Technologies, Wheaton, Illinois) was used to spray the low and high doses of glyphosate at spray rate of 187 L/ha. Pressure was set at 138 kPa, release height was 36 cm, and forward speed was 3.7 km/h.

The hyperspectral imaging system was set up in the greenhouse where the soybean pots were located. In order to record chronological plant injury response, a series of images were taken after spraying treatment. The time series intervals for imaging remained the same at 4, 24, 48, and 72 h after application. Thus, the total number of sample images was 48. In addition, dark and reference images were taken for the purpose of image calibration. The dark image data were taken with the camera lens completely blocked. The reference scan was taken over a standard diffuse reflectance surface. In this study, a 12×12 in. (30.5×30.5 cm^2) white diffuse reflectance standard panel (Spectralon: SRT-99-100 UV–VIS–NIR Diffuse Reflectance Target, LabSphere Inc.) was used to take reference reflectance data. The dark image was taken once for each imaging session. The reference image was taken for every pot sample in order to minimize the influence of ambient outdoor natural light variations. During image acquisition, direct sun light was blocked with a large placard board ($\sim 4 \times 8$ ft). Tungsten lights were used as the illumination source. Thus, both the reference and sample images were acquired under the same lighting condition, i.e., direct halogen light plus diffuse sunlight.

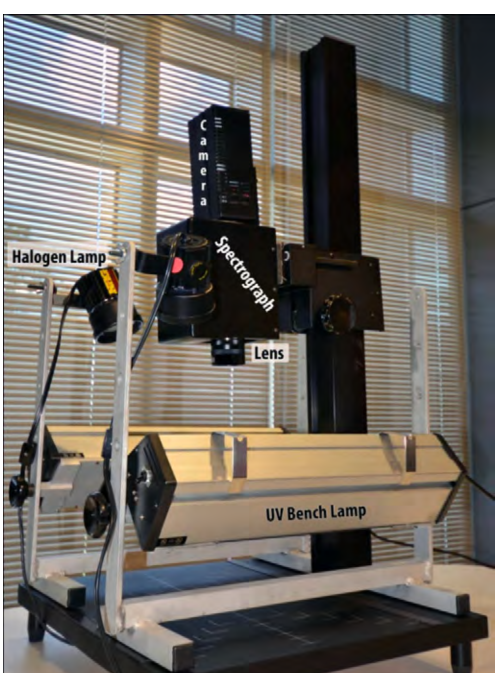

Fig. 1. Illustration of the visible near-infrared hyperspectral imaging system.

2.3. Hyperspectral image processing

Each raw hyperspectral image was pre-processed with a series of steps including: data format conversion; wavelength assignment; scene calibration to percentage reflectance; spectral noise removal; and band subset. In the pre-process step, the data format was converted from integer to floating point. Each band was assigned with a wavelength which was calibrated previously.

The imaging sensor recorded only raw digital counts of reflectance; therefore, the previously recorded dark and reference images were used to convert the raw digital counts to percent reflectance. For reflectance calibration, the following equation was used:

$$Reflectance_\lambda = \frac{S_\lambda - D_\lambda}{R_\lambda - D_\lambda} \times 100\% \quad (1)$$

where $Reflectance_\lambda$ is the reflectance at wavelength λ; S_λ is the sample intensity at wavelength λ; D_λ is the dark intensity at wavelength λ; R_λ is the reference intensity at wavelength λ. A Savitzky–Golay filter was used to remove the data noise. After preprocessing, the calibrated image had 171 bands with wavelength range from 400 to 900 nm. The average bandwidth was 2.92 nm.

From each calibrated image, the reflectance of soybean plants needed to be extracted for further analysis. To do this, an image spectral threshold process was first used to build a mask image with plants in the foreground and the rest in the background. The threshold process used one image band (550 nm) of the hyperspectral image. An NDVI image was also created using two bands (750 nm for NIR, 650 nm for red). The mask image and NDVI image were intercepted to create a region of interest (ROI) for the soybean plants. Finally, the pure plant canopy reflectance of each sample was averaged and extracted over the ROI (Fig. 2).

2.4. Calculation of vegetation index of whole canopy reflectance

Many vegetation indices have been designed and implemented in various applications in the past (Jackson and Huete, 1991). In this study, eight narrow-band vegetation indices were calculated using the measured spectral reflectance of the plant canopy. For simplicity, these indices are all based on two-band calculations and listed in Table 1. The bands used in the calculation include: Green, 551 nm, Red, 676 nm, and NIR, 751 nm. These wavelengths correspond to maximum green reflectance (551 nm), maximum chlorophyll absorption (676 nm) and the maximum chlorophyll reflectance (751 nm) recorded by the hyperspectral sensor.

2.5. Modified approach to calculation of spectral derivatives

Instead of using soybean canopy reflectance to compute derivatives directly, a modified approach was designed in this study. For each sample reflectance, it was normalized based on the following equation:

$$NR_\lambda = \frac{R_\lambda}{Control_\lambda} \tag{2}$$

where R_λ is the calibrated mean sample reflectance at wavelength λ; $Control_\lambda$ is one calibrated control sample reflectance at wavelength λ; NR_λ is the control normalized sample reflectance. The *Control* reflectance was from the same time interval as the *R* reflectance. Only one control sample was used for the normalization step. The rest of the controls were still treated as regular samples. Through this calculation, the sample reflectance was normalized band-by-band by the control sample. The motivation of the process was to offset the baseline signal from the control sample in order to maximize the plant stress response due to the glyphosate application. Since there were only four control measurements for each time interval, it was desirable to maintain this number in the subsequent statistical analysis. Instead of using full canopy reflectance from the control sample for normalization, the hyperspectral image for the control sample was divided into two parts, and each half retained half of the plant canopy. Reflectance from one half of the plant was treated as a regular control sample. Reflectance from the other half of the plant was used for the normalization calculation.

As discussed previously, spectral derivatives could be robust spectral estimates of agronomic parameters of plants since they tend to reduce the variability due to changes in illumination or background reflectance properties. This study computed the first derivative of the above control-normalized sample reflectance. Since the spectral data were discretely sampled for each wavelength based on the predetermined spectral sampling interval, the derivative spectra was calculated with the following differential method:

$$NR'_\lambda = \frac{\Delta NR_\lambda}{\Delta W} = \frac{NR_{\lambda+1} - NR_{\lambda-1}}{W_{\lambda+1} - W_{\lambda-1}} \tag{3}$$

where W_λ is the wavelength number (nm) at wavelength λ. $\lambda + 1$ indicates the next image band of the band at wavelength λ, and vice versa for $\lambda - 1$.

2.6. Statistical analysis

Eight narrow-band vegetation indices from canopy reflectance were analyzed using the SAS GLM procedure (SAS Institute Inc., Cary, NC). The mean separation of the indices between high, low and 0 (control) doses and between 4, 24, 48, and 72 h after treatment (0.05 confidence probability) were calculated. Moreover, linear discriminant analysis was implemented for each time period after treatment. A leave-one-out cross validation schema was used in the analysis. The discriminant analysis was based on the eight vegetation indices. Four derivative indices were selected from the modified first order derivatives. A similar linear discriminant analysis was also implemented over the four derivative indices.

3. Results and discussion

3.1. Visual assessment of plant injury and observations of reflectance

Fig. 3 shows the status of soybean canopy from the control group at 4 h and 72 h post treatment. Significant growth can be seen in the images. Two new branches have developed during this period (in the middle of each image). The mean canopy reflectance from 4, 24, 48, and 72 h are presented in Fig. 4. The reflectance curves have similar shapes. Reflectance from later hours generally

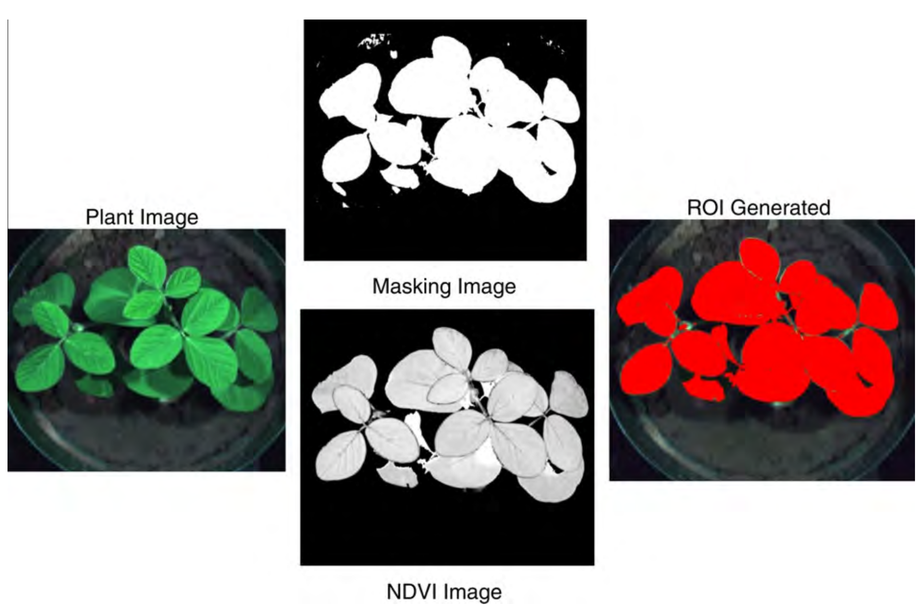

Fig. 2. Illustration of generating region of interest over the soybean plant. The images were generated with the hyperspectral image data with false color composition (R: 650 nm; G: 550 nm; B: 450 nm).

Table 1
Vegetation indices calculated with their references (G: Green, R: Red, NIR: Near-Infrared).

Acronym	Name	Equation	Reference
DVI	Difference Vegetation Index	$DVI = NIR - R$	Tucker (1979)
NDVI	Normalized Difference Vegetation Index	$NDVI = \frac{NIR - R}{NIR + R}$	Rouse et al. (1973)
RI	Redness Index	$RI = \frac{R - G}{R + G}$	Escadafal and Huete (1991)
RVI	Ratio Vegetation Index	$RVI = \frac{NIR}{R}$	Jordan (1969)
SAVI	Soil Adjusted (L = 0.5) Vegetation Index	$SAVI = \frac{NIR - R}{NIR + R + L} \times (1 + L)$	Huete (1988)
TVI	Transformed VI	$TVI = \sqrt{\lvert NDVI + 0.5 \rvert}$	Perry and Lautenschlager (1984)
VNNIR		$VNNIR = \frac{NIR}{NIR + R}$	Pearson and Miller (1972)
VNR		$VNR = \frac{R}{NIR + R}$	Pearson and Miller (1972)

demonstrated elevated green and NIR values, indicating the steady increase in plant vigor. The monotonically increased NIR reflectance coincides with the increase in hours.

For the low dosage treatment group, the new plant growth is moderate. Fig. 5 shows the status of soybean canopy from the low treatment group at 4 h and 72 h post herbicide application. Contrary to the control group, the new leaves that appeared at 4 h did not develop into new branches. There is only a slight increase in size for the new leaves. The inhibition from glyphosate to plant growth is obvious. Another observation over the canopy is that the plant is somewhat withered due to the effect of the herbicide. The mean canopy reflectance for the low dosage treatment group is displayed in Fig. 6. The reflectance curves all have similar shapes. Similar to the control group, the green reflectance gradually increased with the number of increased hours. However, the NIR reflectance displayed a different trend. From 4 h to 48 h the NIR reflectance increased monotonically, which is also similar to the control group. At 72 h the NIR reflectance dropped quickly, showing a decrease in plant vigor due to the herbicide treatment. This information could be used for plant injury assessment. The drawback is that this obvious change happened at 72 h post treatment. It would be preferred if other indicators could be identified for even earlier detection of plant injury.

Plant images of the high dosage treatment group for all time periods are depicted in Fig. 7. No obvious new growth was observed. The new leaves did not grow and plants were all withered. Visible burn spots (Fig. 8) were also observed on the surface of the leaves in the later period of the experiment. Since the experiment was not set up for single leaf measurements, it was difficult to select the same leaf with good views from different time periods.

Fig. 3. Illustration of control plants at 4 h and 72 h post treatment. Development of plant is clearly visible. The images were generated from the hyperspectral image data with false color composition (R: 650 nm; G: 550 nm; B: 450 nm).

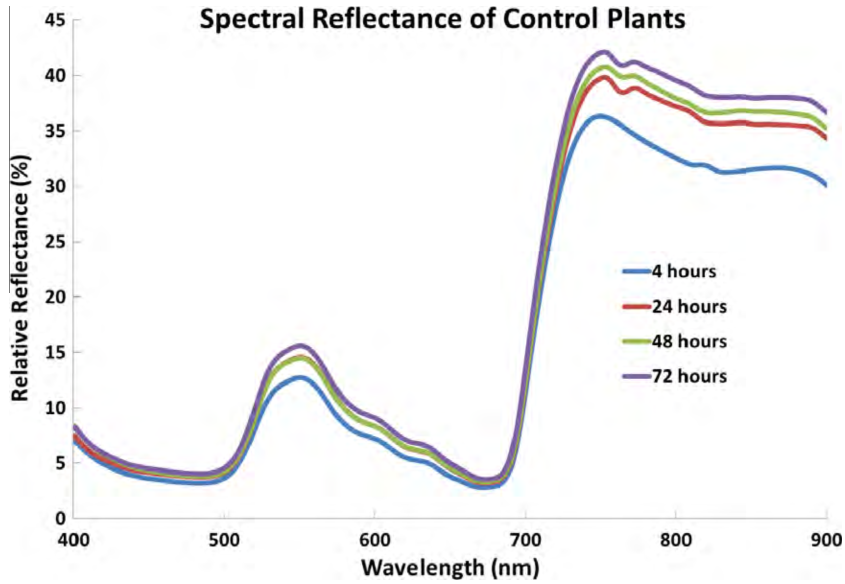

Fig. 4. Time sequence mean reflectance curves for the control group. NIR reflectance is increasing monotonically with the increase of hours.

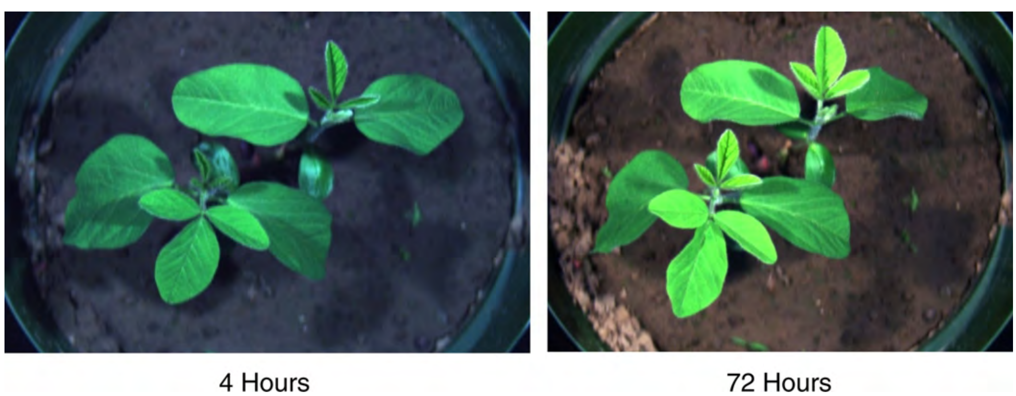

Fig. 5. Illustration of low dosage treatment plants at 4 h and 72 h post treatment. Inhibition of plant growth from the herbicide is obvious. The images were generated from the hyperspectral image data with false color composition (R: 650 nm; G: 550 nm; B: 450 nm).

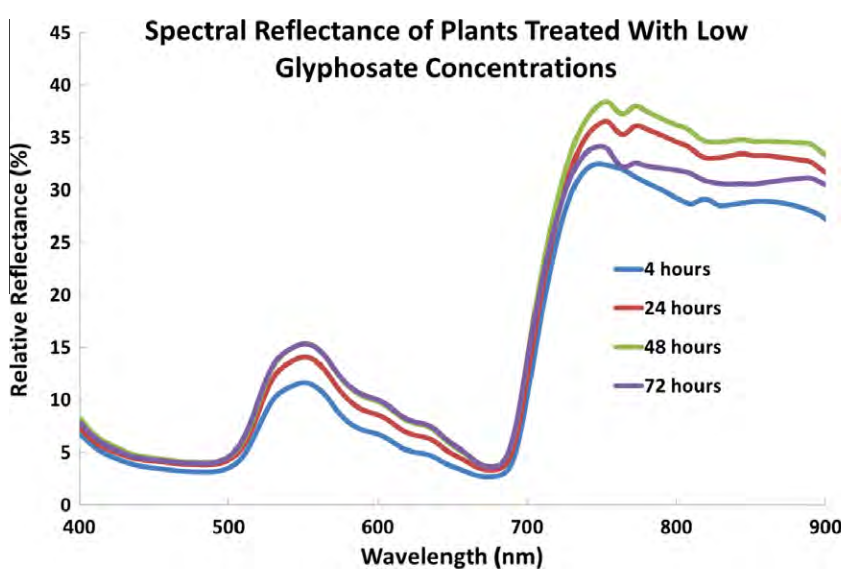

Fig. 6. Time sequence mean reflectance curves for the low dosage treatment group. Note the change in NIR reflectance for 72 h post treatment.

Thus, the leaf image from 24 h was not as clear as the same leaf from other periods. Generally, plant injury due to glyphosate is obvious for the high dosage treatment group, especially for the plants with longer durations after treatment.

The mean canopy reflectance for the high dosage treatment group is displayed in Fig. 9. The reflectance curves from 4, 24, and 48 h were grouped together with similar shapes, while the curve from 72 h detached from the other curves. As for the three curves, from 4, 24, and 48 h, the green reflectance still gradually increased with the number of increased hours. The NIR reflectance increased from 4 h to 24 h. At 48 h it dropped, which is similar to the curve at 72 h from the low dosage treatment group. This trend shows that the NIR reflectance could be used for injury detection for the high treatment group at 48 h post application.

In Fig. 9, the curve from 72 h for the high dosage treatment has higher reflectance values throughout the entire spectrum (400–900 nm). The phenomenon is in contradiction to what was observed for the rest of the experiment. A review of the experiment process revealed that when imaging the high dosage treatment at 72 h, the pots were raised 2 in., which resulted in a shorter imaging distance for those four pots. The purpose of this adjustment was to compensate for canopy coverage in the image due to the limited canopy development for the high dosage treatment group. Consequently, the resulting reflectance curve was elevated. Since this paper focused on using band ratio-based methods for data analysis, which is insensitive to the overall magnitude change of the reflectance curve, it was decided that this group of data would be retained for further data analysis.

3.2. VI statistics

Eight narrow-band vegetation indices from canopy reflectance data were calculated and analyzed. Tables 2–5 show the results of the mean separation of the vegetation indices for 4, 24, 48 and 72 h after treatment, respectively. Table 2 indicates that 4 h after treatment all vegetation indices (except DVI) were not significantly

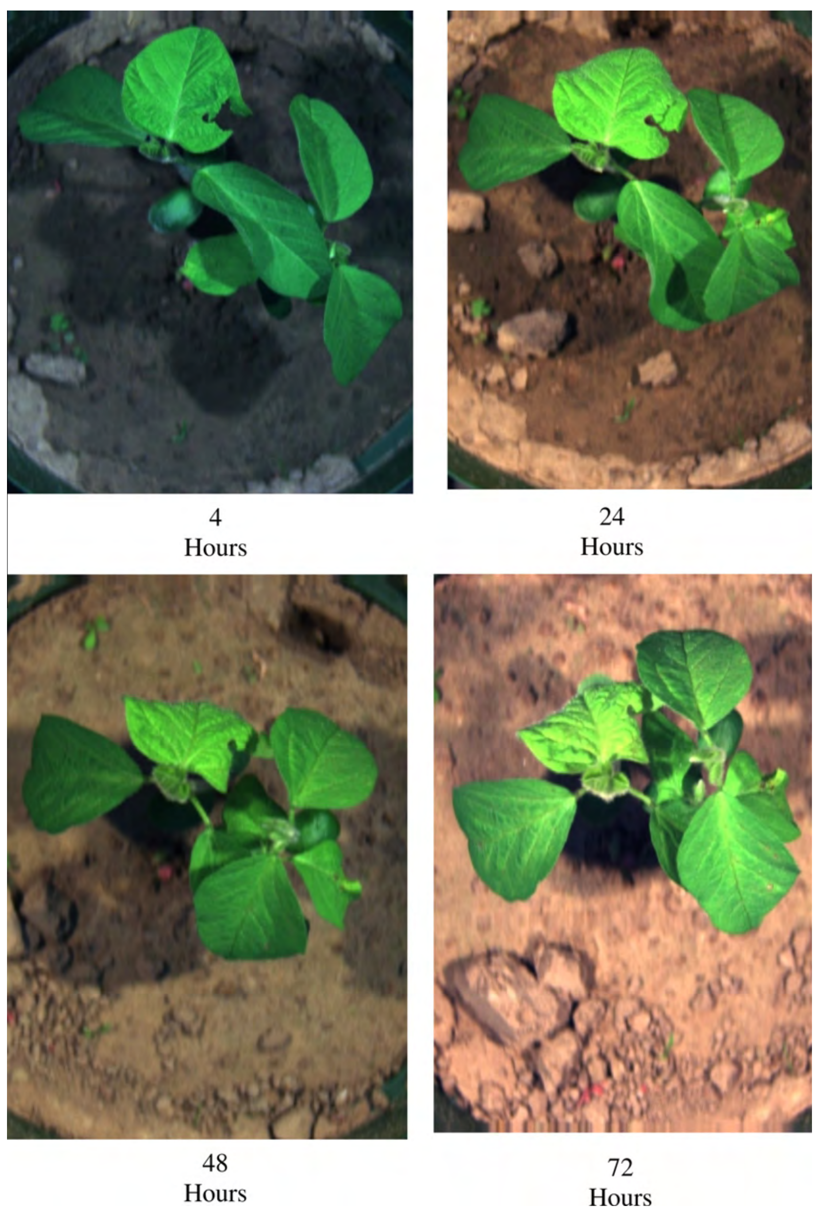

Fig. 7. Illustration of high dosage treatment plants at 4, 24, 48, and 72 h post treatment. Inhibition of plant growth from the herbicide is obvious. The images were generated with the hyperspectral image data with false color composition (R: 650 nm; G: 550 nm; B: 450 nm).

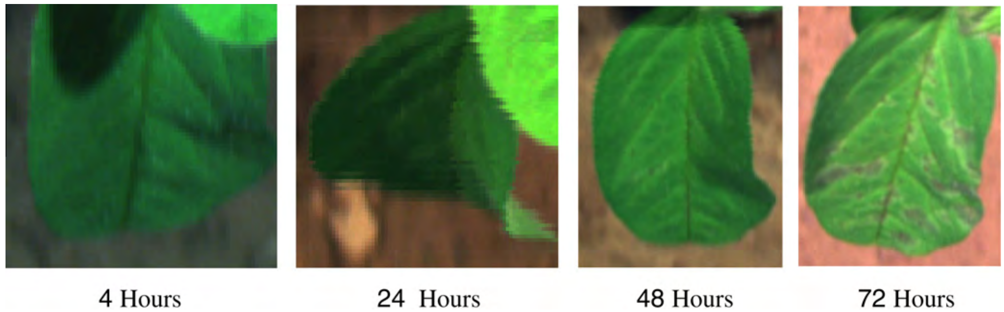

Fig. 8. Observation on one leaf from the high dosage treatment group. The burned spots at 72 h are quite obvious. The images were generated from the hyperspectral image data with false color composition (R: 650 nm; G: 550 nm; B: 450 nm).

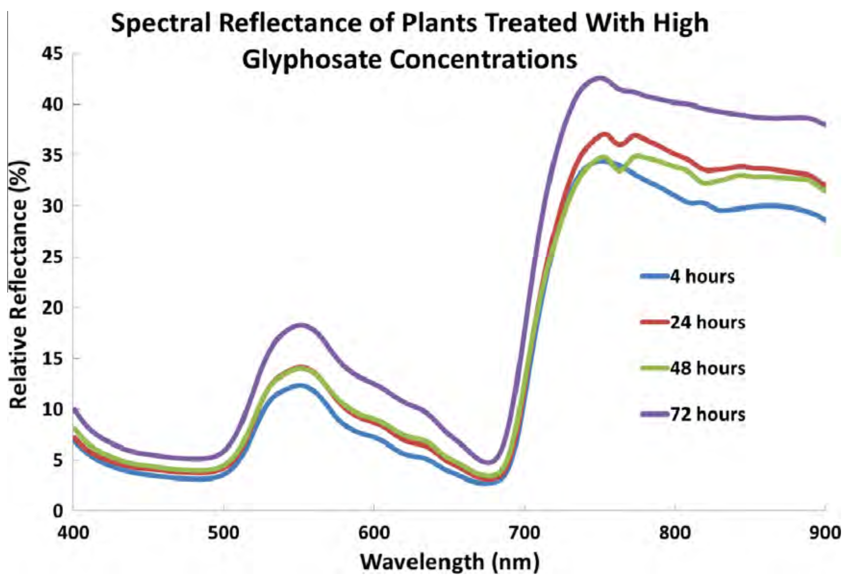

Fig. 9. Time sequence mean reflectance curves for the high dosage treatment group.

different from each other. Table 3 indicates that at 24 h after treatment five indices, NDVI, SAVI, TVI, VNNIR, and VNIR, showed significant difference between the control and low dosage groups. It also indicates that the high dosage group was different from the other two groups at 24 h. At 48 h after treatment (Table 4), all indices (except RI) were significantly different between the control and high dosage groups. At the same time, the low dosage group was different from the other two groups with the same indices. Lastly, at 72 h after treatment (Table 5), the control group was significantly different from the treatment groups (low and high) with five indices, NDVI, RVI, SAVI, TVI, and VNNIR. To summarize the results, at 4 h after treatment it was difficult to differentiate the treatment groups with the vegetation indices. Starting from 24 h after treatment, four indices, NDVI, SAVI, TVI, and VNNIR, demonstrated consistent performance in separating the treatment groups. At 24 h, the control and low dosage groups were significantly different from each other. At 48 h, the control and high dosage groups were significantly different. At 72 h, the control group was significantly different from all the treatment groups. Also at this time there was no difference between the low and high dosage groups while the other time periods exhibited differences.

Tables 6–8 show the results of the mean separation of the vegetation indices from 4, 24, 48, to 72 h after control, low dosage, and high dosage treatment, respectively. First, the control group results in Table 6 indicate that all vegetation indices (except VNR) were not significantly different from 4 h to 72 h. Secondly, for the low dosage treatment group in Table 7, the four indices identified in the previous step, NDVI, SAVI, TVI, and VNNIR showed that 24 and 72 h were significantly different from 4 h. The 48 h results were different from the other groups but the difference was not significant. Indices from 24 and 72 h were not different from each other. Lastly, for the high dosage treatment in Table 8, four indices

Table 2
Mean separation of the vegetation indices 4 h after treatment.[A]

Dose	DVI	NDVI	RI	RVI	SAVI	TVI	VNNIR	VNR
Control	33.449[a]	0.855179[a]	−0.63558[a]	12.8405[a]	1.266521[a]	1.16412[a]	0.927589[a]	0.072411[a]
Low	29.802[b]	0.847595[a]	−0.62610[a]	12.1638[a]	1.253560[a]	1.16085[a]	0.923798[a]	0.076202[a]
High	31.63[ab]	0.851921[a]	−0.63676[a]	12.5558[a]	1.260882[a]	1.16272[a]	0.925960[a]	0.074040[a]

[A] Mean is not significantly different with the same letter at 0.05 level.

Table 3
Mean separation of the vegetation indices 24 h after treatment.[A]

Dose	DVI	NDVI	RI	RVI	SAVI	TVI	VNNIR	VNR
Control	36.549^{a}	0.849220^{a}	−0.63577^{a}	12.2837^{a}	1.25917^{a}	1.16156^{a}	0.924610^{a}	0.075390^{b}
Low	33.193^{a}	0.833335^{b}	−0.61849^{a}	11.0123^{a}	1.23446^{b}	1.154699^{b}	0.916667^{b}	0.083333^{a}
High	33.804^{a}	0.842954^{ab}	−0.63602^{a}	11.7713^{a}	1.2488^{ab}	1.15885^{ab}	0.92148^{ab}	0.07852^{ab}

[A] Mean is not significantly different with the same letter at 0.05 level.

Table 4
Mean separation of the vegetation indices 48 h after treatment.[A]

Dose	DVI	NDVI	RI	RVI	SAVI	TVI	VNNIR	VNR
Control	37.376^{a}	0.847632^{a}	−0.62385^{a}	12.1415^{a}	1.25717^{a}	1.16087^{a}	0.92382^{a}	0.07618^{b}
Low	34.658^{ab}	0.824874^{ab}	−0.61453^{a}	10.5008^{ab}	1.22273^{ab}	1.1510^{ab}	0.91244^{ab}	0.0876^{ab}
High	31.325^{b}	0.819014^{b}	−0.60397^{a}	10.0838^{b}	1.21261^{b}	1.14848^{b}	0.90951^{b}	0.09049^{a}

[A] Mean is not significantly different with the same letter at 0.05 level.

Table 5
Mean separation of the vegetation indices 72 h after treatment.[A]

Dose	DVI	NDVI	RI	RVI	SAVI	TVI	VNNIR	VNR
Control	38.550^{a}	0.843957^{a}	−0.62801^{b}	11.8192^{a}	1.25221^{a}	1.15929^{a}	0.92198^{a}	0.07802^{b}
Low	30.473^{a}	0.805404^{b}	−0.6188^{ab}	9.3141^{b}	1.19155^{b}	1.14253^{b}	0.90270^{b}	0.09730^{a}
High	37.838^{a}	0.800282^{b}	−0.58851^{a}	9.0634^{b}	1.18779^{b}	1.14028^{b}	0.90014^{b}	0.09986^{a}

[A] Mean is not significantly different with the same letter at 0.05 level.

Table 6
Mean separation of the vegetation indices 4, 24, 48, and 72 h for controls.[A]

Hours after treatment	DVI	NDVI	RI	RVI	SAVI	TVI	VNNIR	VNR
4	33.45^{a}	0.8552^{a}	−0.636^{a}	12.841^{a}	1.2665^{a}	1.1641^{a}	0.9276^{a}	0.0724^{a}
24	36.55^{a}	0.8492^{a}	−0.636^{a}	12.284^{a}	1.2592^{a}	1.1616^{a}	0.9246^{a}	0.0754^{b}
48	37.38^{a}	0.8476^{a}	−0.624^{a}	12.142^{a}	1.257^{a}	1.1609^{a}	0.9238^{a}	0.0762^{b}
72	38.55^{a}	0.8440^{a}	−0.628^{b}	11.820^{a}	1.252^{a}	1.1593^{a}	0.9220^{a}	0.0780^{b}

[A] Mean is not significantly different with the same letter at 0.05 level.

Table 7
Mean separation of the vegetation indices 4, 24, 48, and 72 h after low dosage treatment.[A]

Hours after treatment	DVI	NDVI	RI	RVI	SAVI	TVI	VNNIR	VNR
4	29.80^{b}	0.8476^{a}	−0.626^{a}	12.164^{a}	1.2536^{a}	1.1609^{a}	0.9238^{a}	0.0762^{a}
24	33.19^{a}	0.8333^{b}	−0.618^{a}	11.012^{a}	1.2345^{b}	1.1547^{b}	0.9167^{b}	0.0833^{a}
48	34.66^{ab}	0.8249^{ab}	−0.615^{a}	10.501^{ab}	1.2227^{ab}	1.1510^{ab}	0.9124^{ab}	0.0876^{ab}
72	30.47^{a}	0.8054^{b}	−0.619^{ab}	9.314^{b}	1.1916^{b}	1.1425^{b}	0.9027^{b}	0.0973^{a}

[A] Mean is not significantly different with the same letter at 0.05 level.

Table 8
Mean separation of the vegetation indices 4, 24, 48, and 72 h after high dosage treatment.[A]

Hours after treatment	DVI	NDVI	RI	RVI	SAVI	TVI	VNNIR	VNR
4	31.63^{ab}	0.8519^{a}	−0.6368^{a}	12.556^{a}	1.2609^{a}	1.1627^{a}	0.9260^{a}	0.0740^{a}
24	33.80^{a}	0.8430^{ab}	−0.636^{a}	11.771^{a}	1.2488^{ab}	1.1589^{ab}	0.9215^{ab}	0.0785^{ab}
48	31.33^{b}	0.8190^{b}	−0.604^{a}	10.084^{b}	1.2126^{b}	1.1485^{b}	0.9095^{b}	0.0905^{a}
72	37.84^{a}	0.8003^{b}	−0.5885^{a}	9.063^{b}	1.1878^{b}	1.1403^{b}	0.9001^{b}	0.0999^{a}

[A] Mean is not significantly different with the same letter at 0.05 level.

NDVI, SAVI, TVI, and VNNIR showed 48 and 72 h were significantly different from 4 h. Also no difference was found between the 48 and 72 h groups. The 24 h result was different from the 4 h treatment as well as the later periods. It displayed a transitional response along the timeline after treatment. Performance from other indices were not as good as the above four indices, i.e., NDVI, SAVI, TVI, and VNNIR. To summarize, the four indices used in this study, demonstrated potential for glyphosate injury detection. Early plant stress caused by the herbicide could be identified at 24 h after treatment. Results from the low and high dosage groups were slightly different with regard to plant response at 24 and 48 h after treatment. At 72 h, these indices clearly showed that the treatment groups were different from those at 4 h. The outcome signifies that canopy reflectance could be an important tool for

Table 9
Summary of discriminant analysis with cross-validation using linear discriminant function. NDVI, SAVI, TVI, and VNNIR were used in the analysis.

	Number of observations classified into treatment			
From treatment	Control	Low	High	Accuracy (%)
(4 hours)				
Control	2	0	2	50
Low	0	1	3	25
High	1	3	0	0
(24 hours)				
Control	2	1	1	50
Low	0	2	2	50
High	1	2	1	25
(48 hours)				
Control	3	1	0	75
Low	1	2	1	50
High	0	2	2	50
(72 hours)				
Control	4	0	0	100
Low	0	3	1	75
High	1	1	2	50

the detection of early plant stress/injury due to glyphosate application.

The four best vegetation indices from the previous mean separation analysis, NDVI, SAVI, TVI, and VNNIR were used in the following linear discriminant analysis. The results are presented in Table 9. In general, classification accuracy for each treatment group increased gradually with longer duration. For example, from 4 to 72 h, accuracy for the control group changed from 50% to 100%. In the same period, accuracy for the low dosage group changed from 25% to 75%, and for the high dosage group, 0% to 50%. If the goal was not to separate the low and high groups, these two treatments could be regarded as one treatment group. In this case the problem became a two-class classification. Consequently the pooled result had 87.5% accuracy for the treatment group for all the periods. At the same time some control samples were classified as treatment, or called false positive. The false positive rate was 22%, 22%, 11%, and 0% for 4, 24, 24, and 72 h periods, respectively. Thus, from the above linear discriminant analysis, it is demonstrated that herbicide damage to the soybean plants could be identified from 4 to 72 h post application with vegetation indices derived from canopy reflectance data. Longer duration of post application tends to have better results with less false positive classification.

3.3. Modified derivative analysis

The calculated mean first derivatives based on the modified approach were plotted in Fig. 10. Derivatives from control, low dosage, and high dosage treatment groups were plotted separately. The noticeable features in the figure are the derivative peaks. These peaks have low magnitudes for the control group. The magnitudes became larger for the low treatment and largest for the high treatment groups. The change in peak magnitude is the result of treatment difference in dosage. For the high dosage treatment group at 72 h, the magnitude change could be the result of the change in imaging conditions. In addition to the peaks, most of the derivatives are distributed horizontally with values close to zero. Naturally, the derivative peaks can be used in the spectral data analysis for plant injury detection.

From Fig. 10, four first derivatives were selected based on the peak responses. The wavelength locations for these derivatives were at 519, 670, 685, and 697 nm. Except for one green wavelength, the other three are all in or near the red edge region. Similar to the vegetation indices, linear discriminant analysis was implemented with the four derivatives. The results are presented in Table 10. The overall classification accuracy for each treatment group had a similar trend to the results from the vegetation indices. The accuracy increased gradually with longer duration, but converged more quickly. For example, from 4 to 72 h, accuracy for the control group changed from 50%, 75%, 100%, to 100%. In the same period, accuracy for the low dosage group changed from 25% to 100% at 24 h and later. For the high dosage group, the accuracy was 75%, 75%, 100%, and 75%. For pooled treatment, the accuracy of treatment group was 87.5%, 100%, 100%, and 100% for the four time periods. The false positive rate was 22%, 11%, 0%, and 0%. Overall, the spectral derivatives demonstrated better detection results than did the vegetation indices for herbicide damage detection with soybean canopy reflectance. Similar to the vegetation indices, the derivatives also had better results with longer duration of post application, as well as with less false positive classification. Starting at 4 h, the treatment groups could be identified. After 24 h and later, the separation between control and treatment became more obvious and also more consistent. Moreover, the derivatives provided even better differentiation among different treatment groups.

It is obvious that the modified derivative analysis generated better results than the analysis based on the vegetation indices. In this study, the canopy reflectance data was extracted from hyperspectral imagery. The hyperspectral imagery was collected in a greenhouse environment. Although artificial light was used as the main source of illumination, the experiment was still influenced by the external sunlight. The derivative approach could minimize the impact of light variation. This is one reason why the derivatives performed better than the vegetation indices. This study used a modified approach to calculate derivatives. The process involved using sample data divided by control data. The motivation for this step was to remove the influence of the baseline measurement. In this study, the baseline measurement was half canopy reflectance of a control sample. If this method was to be adopted for practical use in the field, ancillary information would be necessary to identify plants not affected by herbicide application. Baseline spectral measurement can then be taken from the healthy plants.

3.4. Further discussion

Another consideration for this study was the relatively small number of samples in each treatment. Since each sample was imaged individually with the hyperspectral sensor, the potential size

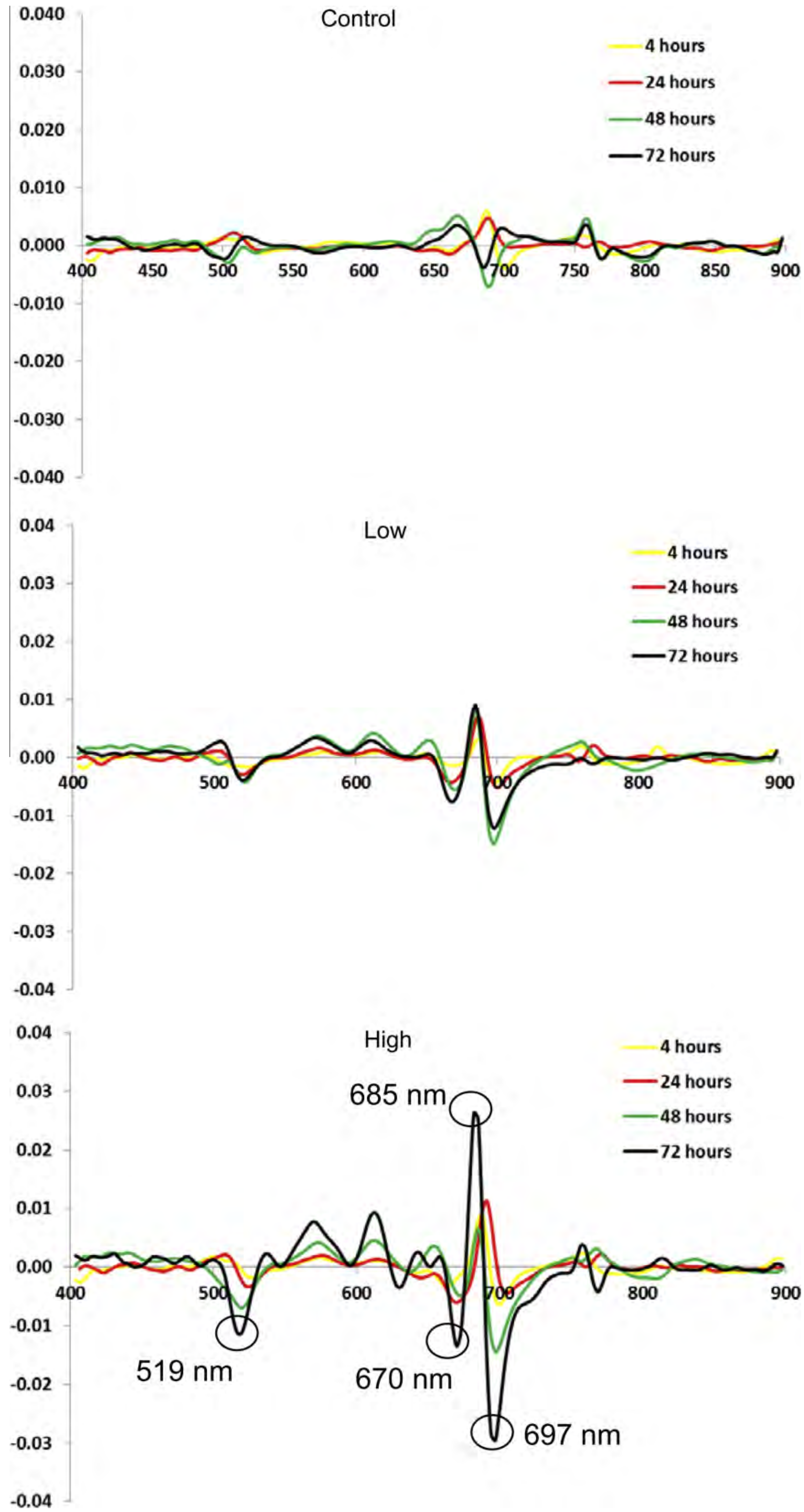

Fig. 10. First derivatives plotted again wavelength. Note the peaks wavelength 519, 670, 685, and 697 nm.

of the hyperspectral image data could be enormous if a large number of samples were used. In addition, large sample numbers increase the complexity of sample preparation, data collection, as well as image data analysis. With the above considerations, this initial experiment took a moderate approach in order to fulfill the research objective. For future research considerations based on the current results, it is recommended more measurement time intervals be used in the first 24 h post application. From a quantitative point of view, it is suggested that more treatment levels be used in the study. Finally to eliminate the influence of out-door light variations, the imaging experiment could be implemented in a dark room environment.

Table 10
Summary of discriminant analysis with cross-validation using linear discriminant function. First derivative indices at 519 nm, 670, 685, 697 nm were used.

	Number of observations classified into treatment			
From treatment	Control	Low	High	Accuracy (%)
(*4 hours*)				
Control	2	2	0	50
Low	1	2	1	50
High	0	1	3	75
(*24 hours*)				
Control	3	1	0	75
Low	0	4	0	100
High	0	1	3	75
(*48 hours*)				
Control	4	0	0	100
Low	0	4	0	100
High	0	0	4	100
(*72 hours*)				
Control	4	0	0	100
Low	0	4	0	100
High	0	1	3	75

4. Summary and conclusions

In order to assess and detect the onset of glyphosate injury to soybean plants, a study was conducted to measure the canopy reflectance of soybean plants using a portable hyperspectral image sensor in a greenhouse. The soybean plants were subjected to low dosage (0.086 kg ae/ha) and high dosage (0.86 kg ae/ha) treatments that were compared with controls. Hyperspectral images were taken at 4, 24, 48, and 72 h post application. The reflectance data was then analyzed with vegetation indices and with modified spectral derivatives. Four vegetation indices, NDVI, SAVI, TVI, and VNNIR, were found significant in detecting plant injury. With linear discriminant analysis, these indices could identify crop injury at 24 h after application, at which time visual inspection could not distinguish between glyphosate injured and non-treated plants. It was also found that the VIs had difficulty separating the treatment groups with different dosages. The modified derivative analysis produced much better results than the vegetation indices. The first derivatives (at wavelength 519, 670, 685, and 697 nm) could potentially differentiate crop injury at 4 h after treatment. From 24 h and beyond, the detection became quite obvious. Moreover, the derivatives demonstrated the ability to separate treatment groups with different dosages. It is concluded that hyperspectral imaging of plant canopy reflectance could be a useful tool for early detection of soybean crop injury due to glyphosate application, and that the modified spectral derivative analysis proved to be better at detecting this than were the vegetation indices. For future studies, it is suggested that more herbicide treatment levels and shorter imaging intervals be used to track canopy reflectance changes in the plant injury process.

Acknowledgements

Thanks to Mr. Efren Ford and Mr. Richard Horton for technical assistance in raising plants and making herbicide applications, Mr. Jason Weick for assistance with plant reflectance data acquisition, and Mr. Hailong Huang for image data processing and figure preparation. Special thanks to Mr. Russell Kincaid for image data acquisition and processing.

References

Bellaloui, N., Reddy, K.N., Zablotowicz, R.M., Mengistu, A., 2006. Simulated glyphosate drift influences nitrate assimilation and nitrogen fixation in non-glyphosate-resistant soybean. J. Agric. Food Chem. 54, 3357–3364.
Center for Food Safety, 2008. Agricultural Pesticide Use in U.S. Agriculture. <http://www.centerforfoodsafety.org/pubs/USDANASSBackgrounder-Final.pdf>.
Ding, W., Reddy, K.N., Krutz, L.J., Thomson, S.J., Huang, Y., Zablotowicz, R.M., 2011a. Biological responses of soybean and cotton to aerial glyphosate drift. J. Crop Improv. 25, 291–302.
Ding, W., Reddy, K.N., Zablotowicz, R.M., Bellaloui, N., Bruns, H.A., 2011b. Physiological responses of glyphosate-resistant and glyphosate-sensitive soybean to aminomethylphosphonic acid, a metabolite of glyphosate. Chemosphere 83, 593–598.
Escadafal, R., Huete, A.R., 1991. Étude des propriétés spectrales des sols arides appliquée à lamélioration des indices de vegetation obtenus par télédection. CR Acad. Sci. Paris 312, 1385–1391.
Estep, L., Carter, G.A., 2005. Derivative analysis of AVIRIS data for crop stress detection. Photogramm. Eng. Remote Sens. 71, 1417–1421.
Gong, P., Ru, R.L., Biging, G.S., 2003. Estimation of forest leaf area index using vegetation indices derived from hyperion hyperspectral data. IEEE Trans. Geosci. Remote Sens. 41, 1355–1362.
Haboudane, D., Miller, J.R., Tremblay, N., Zarco-Tejada, P.J., Dextraze, L., 2002. Integrated narrow-band vegetation indices for prediction of crop chlorophyll content for application to precision agriculture. Remote Sens. Environ. 81, 416–426.
Henry, W.B., Shaw, D.R., Reddy, K.R., Bruce, L.M., Tamhankar, H.D., 2004. Remote sensing to detect herbicide drift on crops. Weed Technol. 18, 358–368.
Huang, Y., Thomson, S.J., Ortiz, B.V., Reddy, K.N., Ding, W., Zablotowicz, R.W., Bright, J.R., 2010. Airborne remote sensing assessment of the damage to cotton caused by spray drift from aerially applied glyphosate through spray deposition measurements. Biosyst. Eng. 107, 212–220.
Huang, Y., Thomson, S.J., Molin, W.T., Reddy, K.N., Yao, H., 2012. Early detection of soybean plant injury from glyphosate by measuring chlorophyll reflectance and fluorescence. J. Agric. Sci. 4, 117–124.
Huete, A.R., 1988. A soil-adjusted vegetation index (SAVI). Remote Sens. Environ. 25, 295–309.
Jackson, R.D., Huete, A.R., 1991. Interpreting vegetation indices. Prev. Vet. Med. 11, 185–200.
Jordan, C.F., 1969. Derivation of leaf area index from quality of light on the forest floor. Ecology 50, 663–666.
Pearson, R.L., Miller, L.D., 1972. Remote mapping of standing crop biomass for estimation of the productivity of the shortgrass prairie, Pawnee National Grasslands, Colorado. In: Proc. 8th International Symposium on Remote Sensing of the Environment, vol. 2, pp. 1355–1379.
Perry, C.R., Lautenschlager, L.F., 1984. Functional equivalence of spectral vegetation indices. Remote Sens. Environ. 14, 169–182.
Reddy, K.N., Ding, W., Zablotowicz, R.M., Thomson, S.J., Huang, Y., Krutz, L.J., 2010. Biological responses to glyphosate drift from aerial application in non-glyphosate-resistant corn. Pest. Manage. Sci. 66, 1148–1154.
Rouse, J.W., Haas, R.H., Schell, J.A., Deering, D.W., 1973. Monitoring vegetation systems in the Great Plains with ERTS. In: Third ERTS Symposium, NASA SP-351, vol. 1. NASA, Washington, DC, pp. 309–317.
Rowland, C.D., 2000. Crop Tolerance to Non-Target and Labeled Herbicide Applications. MS Thesis, Department of Plant and Soil Sciences, Mississippi State University, Mississippi State, Mississippi, USA.
Smith, K.L., Steven, M.D., Colls, S.S., 2004. Use of hyperspectral derivative ratios in the red-edge region to identify plant stress response to gas leaks. Remote Sens. Environ. 92, 207–217.
Thelen, K.D., Kravchenko, A.N., Lee, C., 2004. Use of optical remote sensing for detecting herbicide injury in soybean. Weed Technol. 18, 292–297.
Thorp, K., Tian, L., Yao, H., Tang, L., 2004. Narrow-band and derivative-based vegetation indices for hyperspectral data. Trans. ASAE 47 (1), 291–299.

Tsai, F., Philpot, W., 1998. Derivative analysis of hyperspectral data. Remote Sens. Environ. 66, 41–51.
Tucker, C.J., 1979. Red and photographic infrared linear combinations for monitoring vegetation. Remote Sens. Environ. 8, 127–150.
Yao, H., Tian, L., 2003. A genetic algorithm-based selective principal component analysis (GA-SPCA) method for high dimensional data feature extraction. IEEE Trans. Geosci. Remote Sens. 41, 1469–1478.
Yao, H., Hruska, Z., Kincaid, R., Brown, R.L., Cleveland, T.E., 2008. Differentiation of toxigenic fungi using hyperspectral imagery. Sens. Instrum. Food Qual. Saf. 2, 131–224.
Ye, X., Sakai, K., Okamoto, H., Garciano, L.O., 2008. A ground-based hyperspectral imaging system for characterizing vegetation spectral features. Comput. Electron. Agric. 63, 13–21.